Nuclear Instruments and Methods 180 (1981) 93–103

A VERSATILE DETECTION SYSTEM FOR A BROAD RANGE MAGNETIC SPECTROGRAPH

J.C. VERMEULEN *, J. van der PLICHT, A.G. DRENTJE, L.W. PUT and J. van DRIEL
Kernfysisch Versneller Instituut, University of Groningen, 9747 AA Groningen, the Netherlands

Received 14 July 1980

The focal plane detector for the QMG/2 magnetic spectrograph of the Kernfysisch Versneller Instituut is described. It consists of two-dimensional position sensitive proportional detectors and scintillation detectors. The properties of the components of the set-up and of the system as a whole in conjunction with the associated electronics and software are presented. The system allows easy optimization of spectrograph focusing and correction of kinematic effects. The position resolution is about 1 mm for relatively highly ionizing particles (50 MeV α-particles), and slightly worse for low-ionizing particles (50 MeV protons).

1. Introduction

The QMG/2 magnetic spectrograph of the Kernfysisch Versneller Instituut (KVI) has become operational since early 1978 and has been extensively in use for nuclear structure studies since then. The spectrograph has the configuration quadrupole–multipole–dipole–multipole–dipole–dipole and has a horizontal median plane. A complete description of the instrument can be found in refs. [1] and [2]; here we concentrate on the properties of the spectrograph which are important for the focal plane detector. The focal plane is straight, it has a length of 120 cm and its vertical extension varies between 6 cm at the high momentum side and 3 cm at the low momentum side. The dispersion was chosen such that a position resolution of 1.1 mm corresponds to an energy resolution $\Delta E/E = 2 \times 10^{-4}$. The angle of incidence in the focal plane is $(45 \pm 3)^\circ$ over the total energy bite of 20%. By measuring the actual angle of incidence for a particle trajectory one can calculate the corresponding particle scattering angle within the total acceptance angle of 6°. The vertical angle span is also maximum 6°, yielding a maximum solid angle of 10 msr.

The focal plane detector was designed according to the following requirements:

(1) The detector has to be position sensitive in the horizontal direction with a position resolution better than 1 mm for particles incident at 45° and should have an active length of 120 cm. The active height should be 6 cm.

(2) It should be possible to measure the horizontal angle of incidence, with an angular resolution better than 1°.

(3) For particle identification purposes, a position-independent energy loss signal, a total energy signal and a signal proportional to the time-of-flight (TOF) through the spectrograph should be available. It should be possible to detect low-ionizing particles (up to 60 MeV p) as well as high-ionizing particles (e.g. 30 MeV ^{6}Li).

(4) The detector should be position sensitive in the vertical direction in order to inspect the vertical image, and consequently also the vertical object beam spot on target.

(5) The detection efficiency should be essentially 100%, also at counting rates of around 10 kHz.

A preliminary description of the focal plane detection system has already been published [3]. In this paper, we present a full description of the detection system, which has proven to have sufficient flexibility to perform nuclear reaction studies with ejectiles ranging from protons to ^{7}Li (see also ref. [4]).

2. The focal plane detection system

2.1. Outline of the detector set-up

A schematic layout of the focal plane detector is shown in fig. 1. It consists of two nearly identical subsystems beside each other. Each subsystem has an

* Present address: CERN, Geneva, Switzerland.

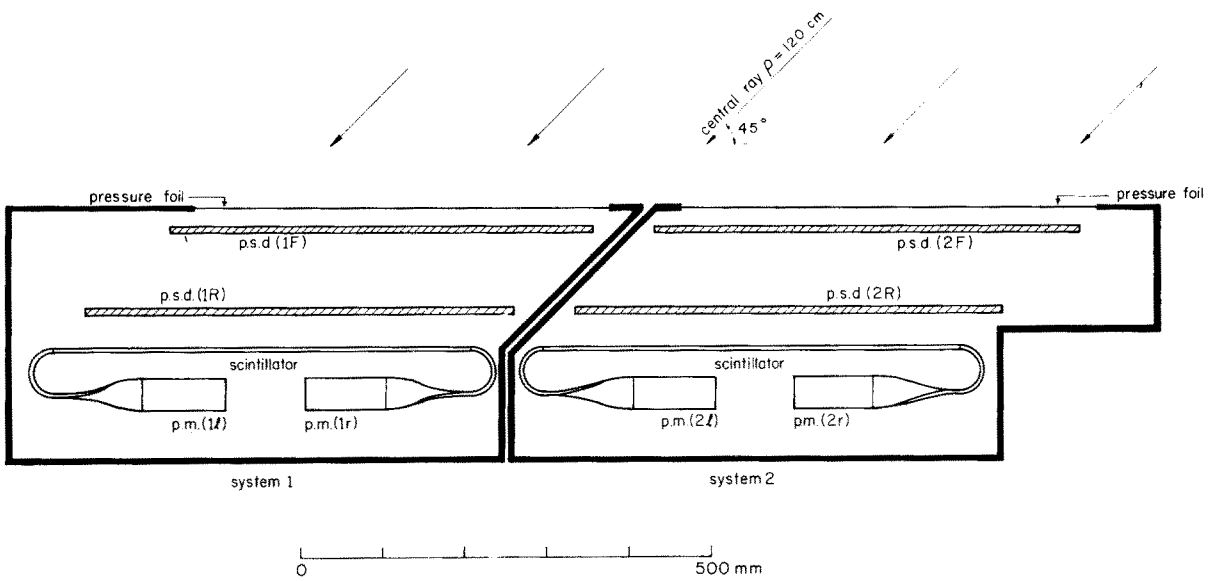

Fig. 1. Schematic layout of the focal plane detection system. F = front detector, R = rear detector; p.s.d. = position sensitive detector; p.m. = photomultiplier (l: left, r: right).

active area of 52 X 6 cm^2 and is contained in an aluminium box. Two two-dimensional position sensitive detectors are placed one behind the other, at a separation of 14 cm measured along the direction of the incident particles. Behind this set-up a scintillation detector is mounted. The position sensitive detectors are gas filled devices, which will be discussed in detail in section 2.2. The scintillation detector is described in section 2.3.

The boxes containing the detectors are placed on a movable support in the vacuum chamber of the spectrograph. The support consists of two arms, one arm for each system. The support as a whole can be moved in the particle direction and in the vertical direction. Each of the two arms can be rotated over a few degrees, making it possible to correct for a curvature in the focal plane which might occur for reactions with strong kinematic effects. The support is adjusted in such a way that the focal plane coincides with the front position sensitive detectors.

Particles enter the detection system through a window of 25 μm thick Kapton foil, which separates the gas inside the box from the spectrograph vacuum and which can maintain a pressure difference of about 1 atm. The gas pressure within the position sensitive detectors is equal to that of the surrounding gas, thus allowing the use of thin detector windows. To minimize energy loss and straggling the surrounding gas can be chosen to be lighter than the counting gas; however, until now it has not been necessary to use this feature. The scintillation detector is operated in the same gas environment as the position sensitive detector. The gas pressure is stabilized by regulation of the gas flow with a needle valve, connected to an electronic feedback unit (Granville–Phillips type 126). The flow is about 50 cc/min.

With the system outlined above we can obtain the following information on the particles entering the detector: (1) the horizontal and vertical position; (2) the horizontal and vertical angle of incidence; (3) the energy loss of the particles in the position sensitive detectors; (4) the total energy of the particles stopped in the scintillator; and (5) the time-of-flight.

2.2. The two-dimensional position sensitive detector

A schematic layout of the position sensitive detector is presented in fig. 2. The detector is essentially a combination of a drift chamber and a resistive wire proportional detector (see also ref. [5]). A vertical, approximately homogeneous electric field is obtained by applying a suitable voltage to very thin horizontal gold strips on the inside of the entrance and exit foil of the detector. Particles which pass through the detector ionize the counter gas. Due to the electric field (about 250 V/cm) the electrons drift downwards (the drift time is about 0.3 μs/cm) towards the anode wire, where charge multiplication occurs. The anode is

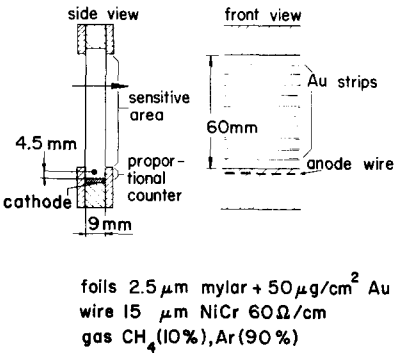

Fig. 2. Schematic layout of the position sensitive detector.

mounted below the focal plane. The rise time of the signal on the wire is determined by the movement of the positive ions away from the anode and by the extension of the electron track, which causes arrival of the electrons in the multiplication region at different times. In the present case both contributions are of the same order and cause a rise time of 50–100 ns, which is long compared with the detector time constant (≈15 ns). The anode wire voltage is chosen such that the detector still operates in the proportional region, so that the total charge collected on the wire is proportional to the energy loss of the particles in the detector. Each of the ends of the anode wire is connected to a charge sensitive preamplifier, which has a very small input impedance. If the capacitance of the detector is neglected Ohm's law gives directly that the charge observed at one end divided by the total charge depends linearly on the position. This relation between the integrated charge at one end divided by the total integrated charge and the position, however, can also be linear when the detector capacitance is not negligible (see e.g. Ford [6] and Vermeulen [4]). Fig. 3 shows an "exploded view" of the position sensitive detector. The detector frame is constructed from G10-material. The anode wire is a 15 μm thick NiCr wire with a resistance of about 3 kΩ. It is centered by guiding it at both ends through a V-groove. The ends of the wire are soldered onto tiny springs, which keep the wire straight during

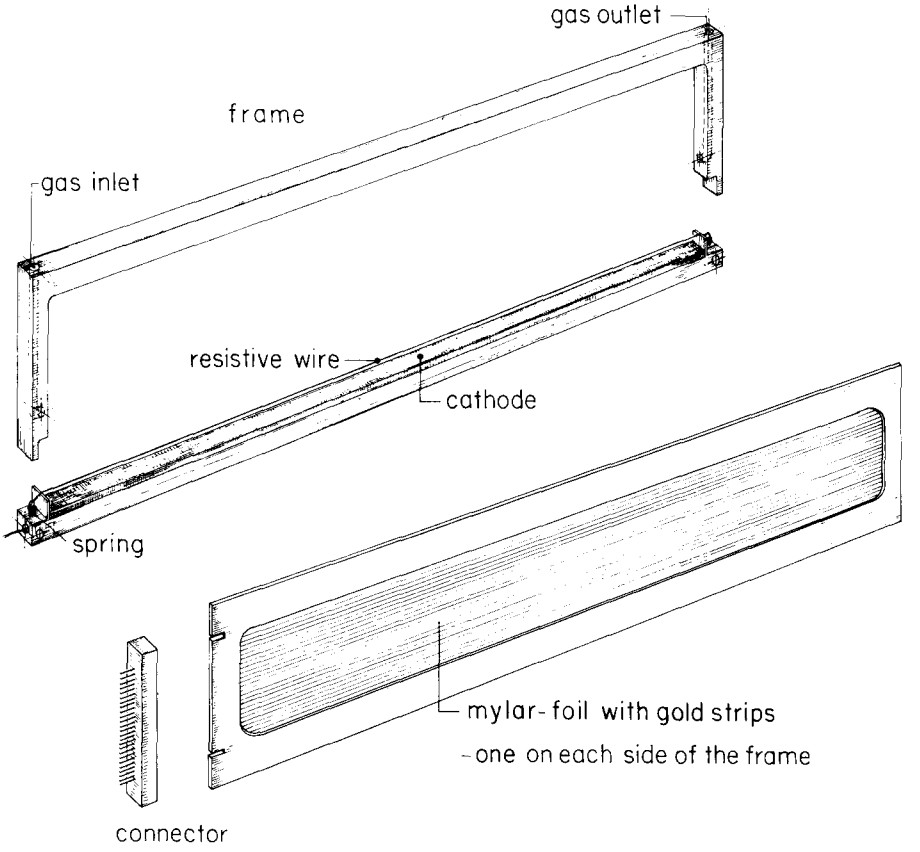

Fig. 3. "Exploded view" of the position sensitive detector.

operation. The cathode consists of a polished flat brass bar, which is mounted 4.5 mm below the anode wire and is connected to ground. The material of the entrance and exit foil is 2.5 μm thick Mylar. The gold strips on the inside of these foils were evaporated through a mask made of nylon wire, after cleaning the foils by means of a glow discharge. The strips are connected via a print connector with a resistive voltage divider. The strips have a width of 1.5 mm and a distance between each other of 1 mm, whereas their thickness is about 50 μg/cm^2. The advantages of this detector design are:

(1) since the particles loose very little energy in the foils with gold strips, the transmission of the detector is essentially 100%, which cannot be achieved by using wires in stead of gold strips.

(2) For relatively weak ionizing particles (e.g. 60 MeV protons) statistical fluctuations of the ionization density along the inclined particle track might cause a detoriation of the position resolution, and this effect can be estimated since the active space of the detector is accurately defined by the Mylar foils.

(3) The Mylar foils enable the box to be filled with a lighter gas than the counting gas.

(4) The performance of the detector does not rely on a high stability of gas pressure and gas composition. The drift time is sensitive to these parameters; however, the vertical position, obtained by measuring the drift time, is mainly intended for judging whether no cut-off occurs (see section 1).

(5) The detector is suited for the detection of light particles as well as for heavy ions. In the latter case, particle identification requires a better energy loss resolution. In principle a separate energy loss detector can be placed between the two position sensitive detectors.

(6) The detector can be used with standard electronics. The charge division can easily be performed with software. The relationship between measured and actual position is essentially linear.

2.3. The scintillation detector

The scintillator consists of a 52 X 6 cm^2, 3.2 mm thick piece of NE102A plastic material, which is coupled to two photomultipliers, one at each end, via bent and twisted perspex light guides (fig. 4). In this configuration the light reflects many times before it reaches the photomultipliers. To guarantee total internal reflection, highly polished material has been used rather than reflective paint or aluminium coating, so that light losses are minimal. The parts of the light guides are glued together with ICI Tensol cement no. 7 and to the scintillator material with Eastman 910 glue. The construction of the light guides and the way in which they are coupled to the scintillator guarantees a good light collection [7].

By summing the last but one dynode signals of the two photomultipliers an "energy" signal is obtained, which is, to first order, position independent. By summing both anode signals a time signal is obtained.

2.4. Associated electronics

A block scheme of the electronic set-up is shown in fig. 5. A slow triple coincidence between the two

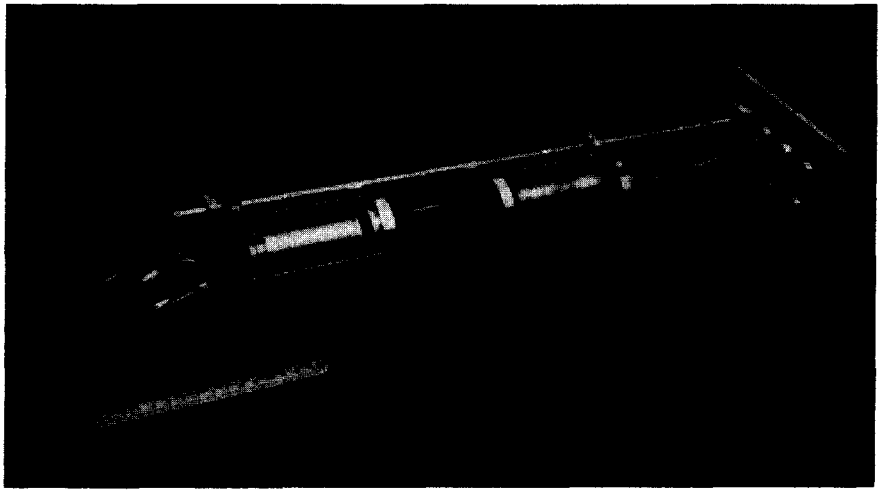

Fig. 4. The scintillation detector.

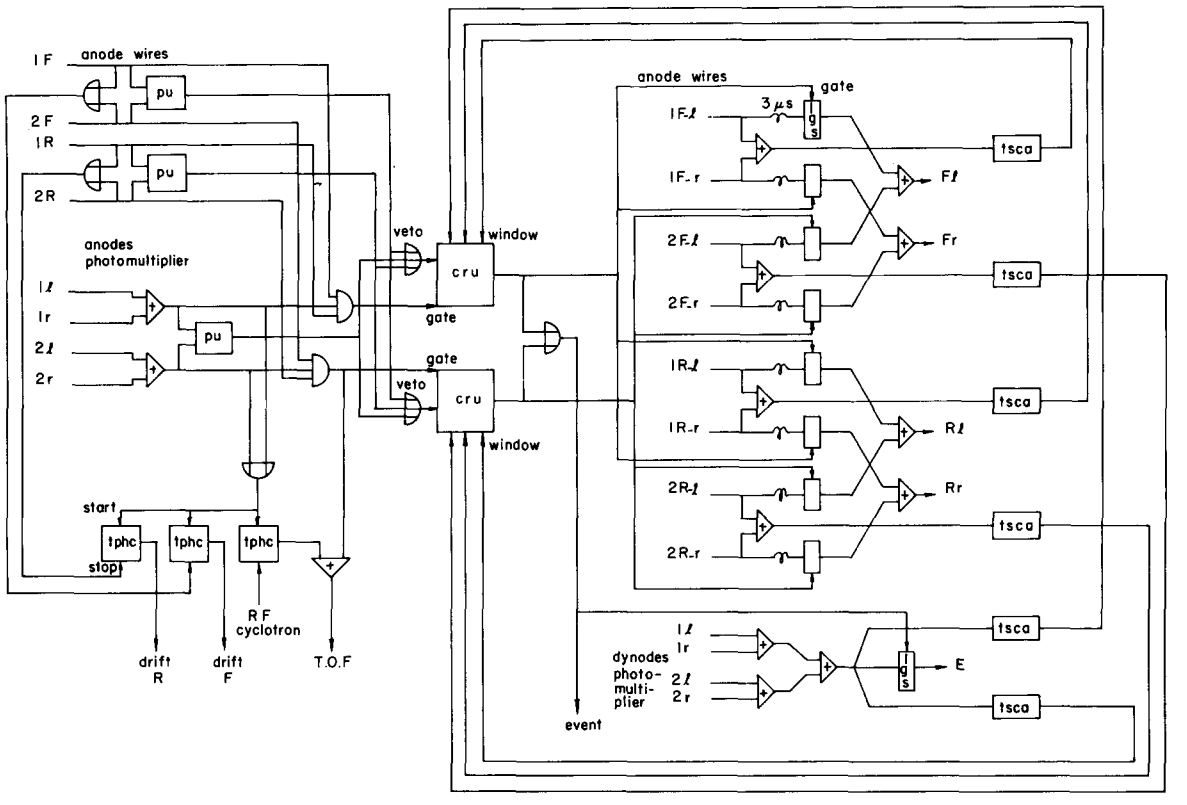

Fig. 5. Block scheme of the electronics set-up for the focal plane detection system: 1, subsystem 1; 2, subsystem 2; F, front; R, rear, 1, left, r, right; cru, coincidence rejection unit; lgs, linear gate stretcher; pu, pile-up gate; tphc, time to pulse-height converter; tsca, timing single-channel analyser.

position sensitive detectors and the scintillator (together constituting one subsystem) is required to define an event (the resolving time is equal to the maximum drift time, which is about 2 μs). The signal used for timing purposes from the position sensitive is the sum of the signals from the charge sensitive preamplifiers (Ortec type 125) connected to the left and right side of the anode wire, thus minimizing walk due to the pulse height differences. Constant fraction timing is applied to these signals as well as to the sum of the left and right photomultiplier anode signals. The time difference between the latter two signals is much smaller than the spread in TOF in the spectrograph and the drift times in the position sensitive detectors, which justifies the summation. The scintillator timing signal is used as the start signal for three time-to-pulse-height converters. The stop signals for the first two are the timing signals of the two position sensitive detectors; the third stop is generated by the cyclotron rf signal. In this way signals indicative of the drift time (i.e. for the vertical position) in the front and the rear detector, and for the TOF through the spectrograph of the detected particle are obtained.

After proper amplification, optimal shaping – 0.25 μs – and delay, the energy signals are stretched by means of linear gate stretchers which are gated by the event signal. To obtain the position information (by means of charge division) of the position sensitive detectors, the signal from the left or the right end of the anode wire and the sum of both are needed. Both summation and division are performed in the computer (see section 2.5). The summation is also performed using hardware, in order to be able to set hardware gates on the energy loss signal. In a similar way, the energy signal of the scintillator can be gated. This preselection is useful in reducing the count rate in the computer in bases with a large contribution from non-interesting events.

An event is defined by eight signals: four anode wire signals, two drift time signals, one TOF signal and one scintillator energy-signal. Event pulses are

generated only if all coincidence requirements for one system are met and all single channel analysers for one system give an output pulse and if no pile-up condition occurs. The logic needed for this is for a large part contained in special units ("cru" in fig. 5). This unit rejects (partially) overlapping pulses, while for non-overlapping pulses which are separated by a time difference smaller than the electronic dead time, only the first pulse can generate an event pulse. The signals are digitized by a Tennelec PACE system which is interfaced to a PDP-15 computer (with 32k memory and EAE-option). The respective signals of both subsystems are mixed before they enter the computer, because our present PACE system can handle at maximum an eight parameter event. The TOF signal is used for the identification of the subsystem: its amplitude is kept smaller than 4 V; for subsystem 2 a pedestal of 4 V is added to it. If both subsystems give pulses within the pile-up inspection time this is seen as a pile-up condition which causes suppression of the event pulse.

The anode wire signals of both subsystems are mixed after the linear gate stretchers to prevent that the noise of the respective detectors is also summed and therefore worsens the signal-to-noise ratio [4]. The photomultiplier dynode signals can be summed before the stretcher, because the resolution is not determined by the signal-to-noise ratio of these signals. The drift time and TOF signals are mixed by coupling the respective timing signals of both subsystems together via or-gates before they enter the time-to-pulse-height converters.

In the detector boxes small capacitors are coupled to the ends of the anode wires and to the photomultiplier anodes and dynodes. This feature facilitates the electronic adjustment and enables the stability of the electronics to be monitored and all the connections to be checked with a pulse generator.

2.5. *Associated software*

The 8 signals per event are handled with the program SPEK (on-line) and PLAY (off-line, events read from magnetic tape) [8]. All calculations are done with 8k-precision; results are converted to the appropriate spectrum length. The programs generate position spectra for the front and rear detectors by dividing the signals from the left end of the anode wire by the respective sums of the signals from both ends. It is possible to correct for offsets and gain differences in the electronic circuitry. Energy loss spectra are obtained by summing the signals from both ends of the anode wires. Spectra of the horizontal and vertical angles of incidence are generated by subtraction of the horizontal and vertical positions in the front and rear detector, respectively. The scaling is such that particles with horizontal and vertical angles of incidence around 45° and 0°, respectively, will give peaks in the middle of the horizontal and vertical angle spectra. All these calculations have to be performed for each event and are therefore programmed as efficiently as possible in assembler language [8]. Within the program the results of these and other calculations are handled as virtual input parameters. The user can easily implement other calculations of this type to suit his particular needs. In the present version it is possible to have a maximum of 16 of such virtual input parameters. On the storage display, we can visualize each combination of two parameters in a so-called *twinkle* plot, in which each point corresponds to an event in the two-dimensional parameter space. It is possible to set one- and two-dimensional software gates on each parameter or combination of parameters. The gates can be combined into specified conditions.

The programs have special features, helpful in judging the focusing of the spectrograph. The trajec-

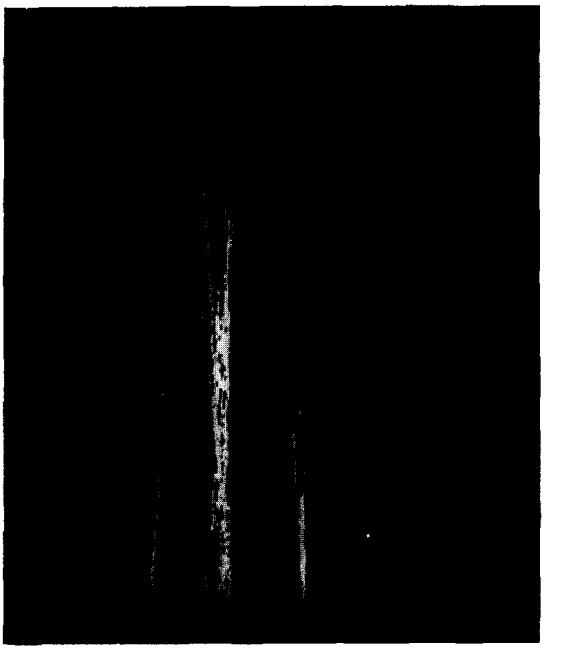

Fig. 6. Particle trajectory plot for the $^{24}Mg(d, {}^{6}Li)^{20}Ne$ reaction (see text for details).

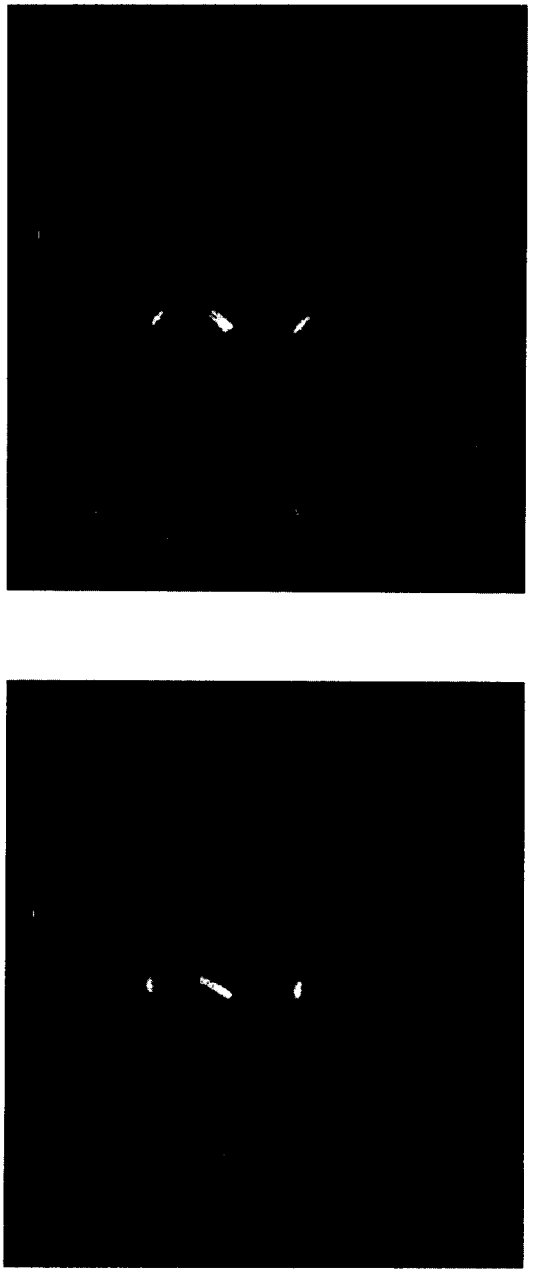

Fig. 7. "Twinkle" plots of horizontal position (horizontal axis) versus horizontal angle of incidence (vertical axis). The corresponding position spectra at the front detector (top) and actual focal plane (bottom) are also shown.

tories of the detected particles can be made visible on the display. An example is shown in fig. 6 for trajectories of ^{6}Li ions, originating from the ^{24}Mg(d, ^{6}Li)^{20}Ne reaction at $E_d = 55$ MeV and $\theta_{lab} = 10°$. The two horizontal lines represent the position in the front (upper line) and the rear (lower line) position sensitive detector of one subsystem. The ^{6}Li ions corresponding to the ground state (right) and of the $E_x = 1.63$ MeV state of ^{20}Ne (left) are focused near the rear detector. Due to a different kinematic factor, ^{6}Li ions from the (d, ^{6}Li) reaction on carbon which is present as a contaminant in the target, are focused in front of the front detector. This is illustrated in fig. 7, where a twinkle-plot of horizontal position (horizontal axis) versus horizontal angle of incidence (vertical axis) is shown for the same case as in the fig. 6, together with the corresponding position spectra. This kind of twinkle plot thus enables the easy judgement and readjustment of focusing, whereas contaminants can be identified easily. The programs allow the calculation of the position spectra in any plane outside the detectors; an example is given in the lower part of fig. 7 which is the result for the actual focal plane.

It is also possible to reject events for which the trajectories pass through a user-defined region anywhere in the displayed area. This feature might be useful to block out reaction particles from target contaminations at their image point, which usually does not coincide with the plane of the first position sensitive detector. Thus, the loss of efficiency for the particles of interest can be minimized.

3. Experimental results

3.1. Measurements with a ^{241}Am source

The detector has been tested extensively with a ^{241}Am α-particle source ($E_\alpha \simeq 5.5$ MeV). The test set-up is shown in fig. 8. The source and a semiconductor detector are placed at either side of the detector. Slits in front of the source and the semiconductor detector and a coincidence requirement between semiconductor and position sensitive detector define the α-particle trajectories to a width of 0.3 mm. The source and the semiconductor detector with the slits can be moved together in the horizontal (parallel to the anode wire) and in the vertical (parallel to the drift field) direction. The counter gas was a 90% Ar, 10% CH_4 mixture at a pressure of about 300 Torr. The voltage applied to the anode wire was 900 V, the drift field strength was about 250 V/cm. The drift time is rather insensitive to variations in the drift field [9] and is about 0.3 μs for one cm. As an example, we show in

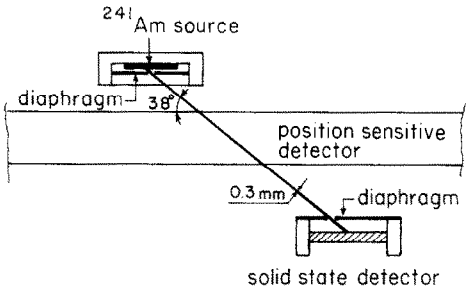

Fig. 8. Schematic layout of the position sensitive detector test set-up.

fig. 9 a part of a horizontal position spectrum for a 90° angle of incidence. The observed fwhm is 0.4 mm; the correction for the finite beam width gives an upper limit for the intrinsic detector resolution of 0.3 mm fwhm. The same intrinsic resolution was found for an angle of incidence of 38°. Fig. 10 shows the deviation of a linear relationship between measured position and α-particle beam position for one half of the detector, which was established by fitting a linear function to the data points for the central part of the detector (positions < 15 cm).

The conclusions drawn from these test measurements are:

(1) the horizontal position resolution for both 90° and 38° horizontal angles of incidence is about 0.3 mm and is independent of the horizontal and vertical position to within 1 cm from the vertical detector edges.

(2) The measured horizontal position is, within the resolution, independent of the vertical position.

(3) The vertical position resolution is better than about 0.3 mm and is independent of the horizontal and vertical position.

(4) The relationship between source position and measured position is linear both in the horizontal and vertical directions. The deviation of the horizontal position is within the spectrograph resolution up to about 5 cm from the edges of the detector.

(5) No indications for efficiency variation have been found. If variations exist at all they are smaller than about 10%.

(6) The energy loss signal shows a slight dependence on the horizontal position; the shift is somewhat smaller than the width of the peak.

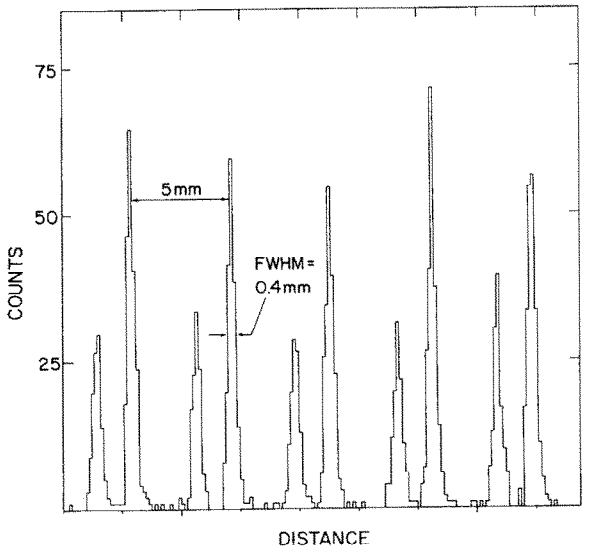

Fig. 9. Position spectrum for 90° angle of incidence as measured with the test set-up of fig. 8 with a double slit (of different size) system at a number of positions 5 mm apart.

3.2. Results with the detector in the focal plane

To obtain the intrinsic position resolution of the detection system for particles at cyclotron energies the following test was performed in the spectrograph: a 6 mm high and 0.5 mm wide slit, mounted 7.6 cm in front of the first detector was exposed to a narrow beam of elastically scattered particles. For 40 and 70 MeV α-particles a resolution of 1.0 mm was found at a pressure of 400–500 Torr. For 55 MeV deuterons an upper limit of 1.5 mm was found at a pressure of 600 Torr; a higher pressure may give a better result. These values include only small contributions due to the energy dispersion of the beam and the finite size of the beam spot on the target.

The intrinsic position resolution of the detector is about equal to the intrinsic resolution of the spectrograph. Therefore no extensive efforts have been made to improve it.

The angular resolution of the detection system was measured for 52 MeV α-particles elastically scattered from a ^{208}Pb target. This was done with a horizontal acceptance of the spectrograph of 0.3° at scattering angles of 14° and 16°, while keeping the position of the spectrograph and the field settings the same. Only the entrance slit was horizontally displaced. The result is shown in fig. 11. The angular resolution of about 1° can be ascribed to the intrinsic position resolution of the detectors and to the angle scattering in the gas between the detectors and the pressure foil, which are giving about equal contributions in this case (the gas pressure was 530 Torr). From com-

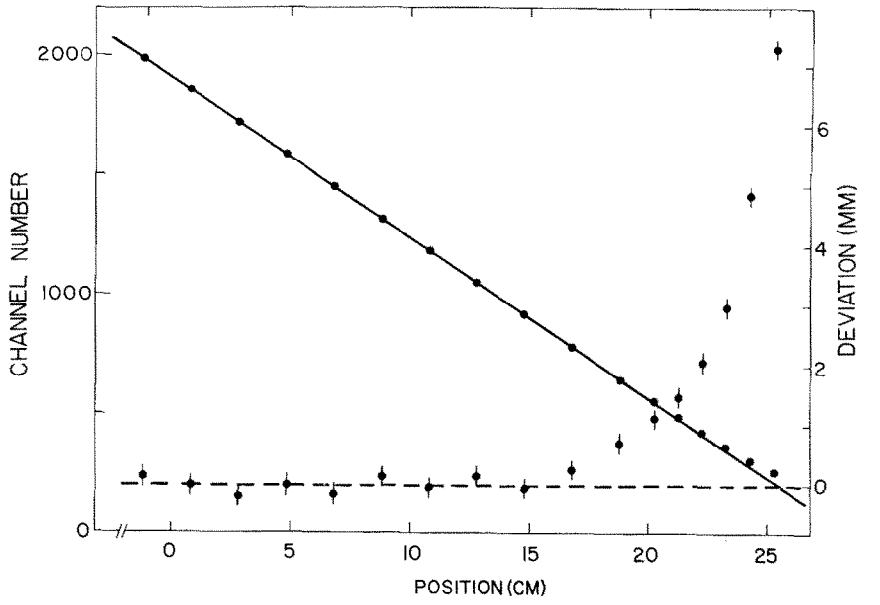

Fig. 10. Measured horizontal position (in channel numbers) as a function of source position for 90° angle of incidence, as measured with the test set-up of fig. 8 for one half of the detector. The source position is relative to the centre of the detector. The full line was fitted to the data points with positions <15 cm. The deviation of the measured position from this line is shown also.

parison of test measurements which yielded well known cross sections, no significant deviation of the efficiency from 100% is observed. Also, by irradiating the detector with a uniform particle distribution a uniform position spectrum was produced so that it is concluded that there are no sharp fluctuations in the efficiency. If in a region of a few millimeters wide, the count rate exceeds a few hundred counts per second, the detection efficiency will decrease. The reason is that the field around the anode wire is locally screened by positive ions for a time of the order of 1 ms after the occurrence of an avalanche. Also the resolution becomes worse due to this effect. Elastic scattering can give rise to these conditions. The detector as a whole, however, can easily be used with count rates higher than 10 000 counts/s.

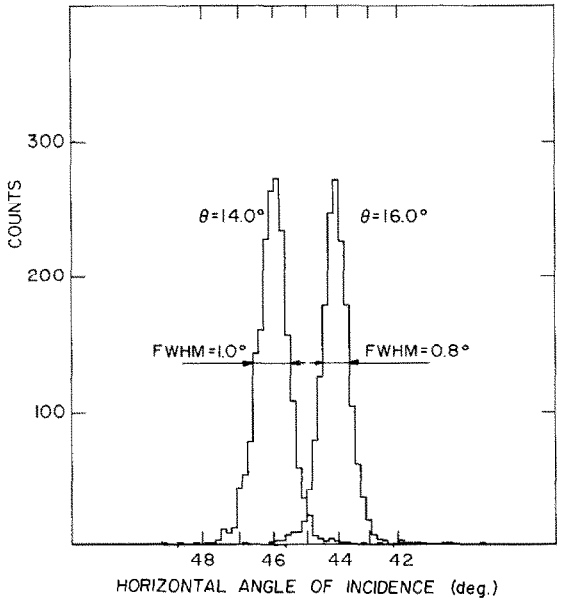

Fig. 11. Angle resolution as measured for 50 MeV α-particles at a spectrograph angular opening of 0.3°.

The focal plane detection system has now been used in a wide variety of experiments. Satisfactory performance was obtained in most cases. Particles detected were protons, deuterons, tritons, ^{3}He-, ^{4}He-, ^{6}Li- and ^{7}Li-ions of energies between 30 and 140 MeV. Satisfactory particle identification could be obtained in nearly all cases by setting software gates on energy loss, scintillator energy or TOF signals or a combination of them. The resolution of the energy loss signal is better than about 30% fwhm; for the scintillator energy signal typically 20% fwhm at a fixed position was found. The scintillator signal is about 20% higher for particles hitting the edges of the scintillator than for particles hitting in the middle, but this effect can be compensated for by software, if necessary. The resolution of the TOF signal is

determined completely by the differences in length of the particle trajectories in the spectrograph, which amount up to ±10% of the central trajectory. In principle, this effect can also be corrected by software. Until now, in most cases the detector gas was a 90% Ar, 10% CH_4 mixture. By choosing a suitable gas pressure and anode wire voltage, the detector contribution to the total position resolution can be minimized. For low-ionizing particles such as 50 MeV protons, a mixture of 90% Ar, 10% C_2H_6 which has a larger gas amplification has been used. The so-called magic gas [10] cannot be used in our case, because it contains the electronegative freon gas which captures electrons during the drift process.

4. Conclusions

We have described a system for the detection of reaction particles and the determination of their position in the 120×6 cm^2 large focal plane of the QMG/2 magnetic spectrograph. The most essential parts of the system are four position sensitive proportional detectors with a length of 50 cm. By applying an electrical drift field the sensitive height of these detectors is as large as 6 cm. For the position determination the charge division method was used. Because of its simplicity, this method was preferred over other readout methods (for a review see e.g. ref. [6]), which might give better position resolution. Furthermore the performance as obtained with this method is sufficient in the present configuration of beam analyzing system and spectrograph which provides a position resolution not better than 1 mm which corresponds to $\Delta E/E = 2 \times 10^{-4}$. An overall detector position resolution of 1 mm was measured for highly ionizing particles, this value worsened to about 1.5 mm for low-ionizing particles.

The system has proven to work satisfactorily for particles with $1 < A < 7$, i.e. protons, deuterons, tritons, ^{3}He, α-particles, ^{6}Li and ^{7}Li ions with various energies have been detected. Only the gas pressure and the anode wire voltage had to be adjusted to obtain optimal performance. The system is in principle also suited for the detection of heavy ions, but for optimal conditions slight modifications or additions may be necessary. An example of this might be the addition of an ionization chamber type detector between the front and rear position sensitive detector [15] (see fig. 1) to get the improvement on the resolution of the ΔE-signal needed for good mass separation (e.g. $\Delta A/A = \frac{1}{15}$). The layout and construction of the system allow such modifications very easily.

Since signals for as many as 8 parameters are obtained from the system, this set-up is very flexible in providing information on the type of detected particles and on the trajectories of the particles through the spectrograph. This information is easily obtained on-line by virtue of a flexible software package.

On basis of the experience with the present detectors a 120 cm long detector is now under construction to cover the whole focal plane.

This work has benefitted much by the intial work of J.W. Smits and W.J. Ockels. We acknowledge the help of D.C.J.M. Hageman, A.S. Keverling Buisman, P. Nammensma and J. van Popta during the testing phase of the detection system. The software described in this paper has been adapted for our purpose by F. Sporrel. The technical staff of the KVI has played an important role in the realization of the detection system. In particular we would like to thank A.H. Bennink, H. Kooi, J.M. Luidens, R. v.d. Ploeg, G.J. Sa, J. Sijbring and W.J. Uytenbogaardt.

This work was performed as part of the research program of the "Stichting voor Fundamenteel Onderzoek der Materie" (FOM), which is financially supported by the "Nederlandse Organisatie voor Zuiver Wetenschappelijk Onderzoek" (ZWO).

References

[1] A.G. Drentje, H.A. Enge and S.B. Kowalski, Nucl. Instr. and Meth. 122 (1974) 485.
[2] A.G. Drentje, R.J. de Meijer, H.A. Enge and S.B. Kowalski, Nucl. Instr. and Meth. 133 (1976) 209.
[3] J. van der Plicht and J.C. Vermeulen, Nucl. Instr. and Meth. 156 (1978) 103.
[4] J.C. Vermeulen, thesis, University of Groningen, unpublished.
J.C. Vermeulen, Nucl. Instr. and Meth., to be published.
[5] W.J. Ockels, J.W. Smits, J.C. Vermeulen and E.J. de Graaf, KVI Annual Report (1975) p. 107.
[6] G.C. Ball, Nucl. Instr. and Meth. 162 (1979) 263; J.C.L. Ford, Nucl. Instr. and Meth. 162 (1979) 277; E.R. Flynn, Nucl. Instr. and Meth. 162 (1979) 305; R.G. Markham, Nucl. Instr. and Meth. 162 (1979) 327; H.W. Fulbright, Nucl. Instr. and Meth. 162 (1979) 341; H.W. Fulbright and J.R. Erskine, Nucl. Instr. and Meth. 162 (1979) 355.

[7] D.G. Grabb, A.J. Dean, J.G. McEwen and R.J. Ott, Nucl. Instr. and Meth. 45 (1966) 301.
[8] J. van Driel and F. Sporrel, KVI Annual Report (1977) p. 82.
[9] F. Sauli, CERN Report no. 77-09 (1977).
[10] P. Rice-Evans, Spark, Streamer, Proportional and Drift Chambers, Richelieu (1974).
[11] H. Stelzer, Nucl. Instr. and Meth. 133 (1976) 409.
[12] R.G. Markham and R.G.H. Robertson, Nucl. Instr. and Meth. 129 (1975) 131.
[13] A. Breskin, G. Charpak, C. Demierre, S. Majewski, A. Policarpo, F. Sauli and J.C. Santiard, Nucl. Instr. and Meth. 143 (1977) 29.
[14] F. Sauli, Nucl. Instr. and Meth. 156 (1978) 147.
[15] P. Nammensma, A. van den Berg, A.G. Drentje and M.N. Harakeh, KVI Annual Report (1979) p. 144.